

Statistical Inference for Scale Mixture Models via Mellin Transform Approach*

Denis Belomestny ^{†1}, Ekaterina Morozova^{‡2}, and Vladimir Panov^{§3}

¹University of Duisburg-Essen, Thea-Leymann-Str. 9, 45127 Essen, Germany

^{2,3}HSE University, Laboratory of Stochastic Analysis and its Applications, Pokrovsky boulevard 11, 109028 Moscow, Russia

November 4, 2022

Abstract

This paper deals with statistical inference for the scale mixture models. We study an estimation approach based on the Mellin – Stieltjes transform that can be applied to both discrete and absolute continuous mixing distributions. The accuracy of the corresponding estimate is analysed in terms of its expected pointwise error. As an important technical result, we prove the analogue of the Berry – Esseen inequality for the Mellin transforms. The proposed statistical approach is illustrated by numerical examples.

1 Introduction

In this paper we consider the problem of statistical inference for multiplicative mixture models. More precisely, given a sample of i.i.d. random variables X_1, \dots, X_n , $n \in \mathbb{N}$, from the multiplicative mixture model of the form

$$X = Y\eta, \tag{1}$$

where Y and η are independent random variables, we aim at estimating the distribution of one of these variables (say, Y) assuming that the law of another random variable (η) is known. For simplicity, we assume that

*The article was prepared in the framework of a research grant funded by the Ministry of Science and Higher Education of the Russian Federation (grant ID: 075-15-2022-325).

[†]denis.belomestny@uni-due.de

[‡]eamorozova@hse.ru

[§]vpanov@hse.ru

both Y and η are almost surely positive, so that η can be viewed as the (stochastic) scaling parameter.

The aforementioned problem can be viewed as the problem of reconstructing the original signal from the contaminated sample and naturally arises in many applications. For instance, the case when η has a standard uniform distribution is known as the multiplicative censoring model and is widely employed in survival analysis (Vardi, 1989). In this context, X corresponds to the time elapsed since the beginning of the disease, whereas Y represents the true survival time (Van Es et al., 2000). The precise estimation of the distribution of Y in this case would help the development of treatment programmes, as well as the assessment of their performance. Another example comes from finance, where the model (1) with normally distributed η and positive Y corresponds to the stochastic volatility model for describing the log-returns of an asset (Van Es et al., 2003, Belomestny and Schoenmakers, 2015).

While certain methods for estimation of the distribution of Y in model (1) already exist, they mostly assume some specific form of the distribution of η . For instance, for the case when η follows a standard uniform distribution, some nonparametric estimation techniques are proposed by Vardi (1989), Asgharian et al. (2012), Brunel et al. (2016). Later, Comte and Dion (2016) and Belomestny et al. (2016) generalise the setting and develop the estimators based on the projection techniques for the case when η follows the uniform distribution symmetric about one and the beta distribution, respectively.

The problem of statistical inference for the multiplicative mixture models can be reduced to the additive deconvolution problem by taking logarithms of both parts in (1) or by taking logarithms of the squares in the alternating case. For the additive models, a wide range of estimation methods is available; see, e.g., Zhang (1990), Meister (2009), Belomestny and Goldenshluger (2021), and numerous references therein. However, as was pointed out by Brunel et al. (2016) and Belomestny and Goldenshluger (2020), this idea leads to several undesired consequences such as inability of estimation at zero and the loss of the information about the sign of the random variable.

For almost all papers mentioned above, the parametric assumption on the distribution of η is essential. The nonparametric case was considered by Belomestny and Goldenshluger (2020) and Miguel, Comte and Johannes (2021), where the kernel-type and series estimators based on the Mellin transform are introduced. However, these papers significantly employ the assumption of absolute continuity of the distributions of Y and η .

In the current paper, we do not impose any restrictions on the class of distributions of η . The only assumption is that the set \mathcal{H}_G determined by (3) from the distribution of η , is non-empty. This assumption holds for a wide class of discrete distributions (see Section 6 for the detailed discussion). Moreover, as we also show in the article, this assumption yields the optimal rate of convergence without any specific restrictions on the class of

the probability density functions (p.d.f.s) of Y .

In order to avoid the assumption of absolute continuity of η , we formulate all results in terms of the distribution functions, assuming for simplicity that both random variables Y and η are a.s. positive. Note that the distribution function of X is equal to

$$F_{\text{mix}}(x) = \int_{\mathbb{R}^+} F\left(\frac{x}{\theta}\right) dG(\theta),$$

where F and G are the cumulative distribution functions (c.d.f.s) of Y and η , respectively. Given observations X_1, \dots, X_n from F_{mix} , we aim to estimate the function $F(x)$, $x \in \mathbb{R}_+$, provided that $G(x)$, $x \in \mathbb{R}_+$, is known.

Our estimation method is based on the Mellin – Stieltjes transform, defined for a function $\varphi : \mathbb{R}_+ \rightarrow \mathbb{R}_+$, which is assumed to be a function of bounded variation over any bounded interval, as

$$\mathcal{M}[\varphi](z) := \int_0^\infty x^{z-1} d\varphi(x), \quad z \in \mathbb{C}. \quad (2)$$

The integral on the right-hand side is known to converge in a vertical strip $\{z \in \mathbb{C} : \text{Re}(z) \in [\alpha_\varphi, \beta_\varphi] =: \mathcal{C}_\varphi\}$, with some $\alpha_\varphi, \beta_\varphi > 0$ (the degenerate case $\alpha_\varphi = \beta_\varphi$ is also possible). Using the properties of the Mellin – Stieltjes transform, we construct an estimator \widehat{F} of F (to be defined in Section 2) and study the accuracy of this estimator at a fixed point $x \in \mathbb{R}_+$ in terms of the expected pointwise error

$$\mathcal{R}^*(\widehat{F}) = \mathcal{R}^*(\widehat{F}; u^\circ, x) := \mathbb{E}\left[\left(\mathcal{R}(\widehat{F}; u^\circ, x)\right)^2\right],$$

where

$$\mathcal{R}(\widehat{F}) = \mathcal{R}(\widehat{F}; u^\circ, x) := x^{u^\circ-1} |F(x) - \widehat{F}(x)|$$

and u° is a technical parameter. We show that under rather mild assumptions on G and F , the estimate \widehat{F} has $1/n$ rate of convergence to F as measured in terms of $\mathcal{R}^*(\widehat{F})$ with n being the sample size.

The paper is organised as follows. In the following section (Section 2) we recall the most important properties of the Mellin – Stieltjes transform and introduce the estimator \widehat{F} for F . In Section 3 we prove the analogue of the Berry – Esseen inequality for the Mellin – Stieltjes transforms (Lemma 3.1), which plays an essential role for establishing the upper bounds for $\mathcal{R}(\widehat{F})$ and $\mathcal{R}^*(\widehat{F})$. The exact statements are given in Section 4, see Theorems 4.1 and 4.2. Next, Section 5 contains the detailed discussion on the subclasses of distribution functions F and G , for which the rate of convergence of the proposed estimators is polynomial. Section 6 is devoted to one of the key assumptions of our estimation procedure, namely, that there exists a line parallel to the imaginary axis such that $\mathcal{M}[G](z) \neq 0$ for any z on this line.

It is shown that the aforementioned assumption is fulfilled, in particular, for any discrete positive distribution separated from zero. Finally, Section 7 contains a numerical example demonstrating the performance of our estimator via a simulation study. Appendix A contains a numerical example of the application of the Berry – Esseen inequality. All proofs are collected in Appendix B.

2 Estimation procedure

Note that the Mellin – Stieltjes transform of F_{mix} is equal to

$$\mathcal{M}[F_{\text{mix}}](z) := \mathbb{E}[X^{z-1}] = \mathcal{M}[F](z) \cdot \mathcal{M}[G](z)$$

for any $z \in \mathbb{C}$ such that both Mellin transforms on the right-hand side are well defined. Since we assume that the distribution of η is known, we can estimate the Mellin transform of F by

$$\widehat{\mathcal{M}[F]}(z) := \frac{1}{n} \sum_{i=1}^n X_i^{z-1} / \mathcal{M}[G](z),$$

at any point $z \in \mathbb{C}$ such that $\mathcal{M}[G](z) \neq 0$. Let us introduce the notation

$$\mathcal{H}_G := \{u \in \mathcal{C}_G : \mathcal{M}[G](u + iv) \neq 0 \quad \forall v \in \mathbb{R}\}. \quad (3)$$

The set \mathcal{H}_G is non-empty in most cases; for instance, as we show in Section 6, for positive discrete distributions, there exists some $\tilde{u} < 1$ such that $(-\infty, \tilde{u}) \subset \mathcal{H}_G$, provided that the distribution is separated from 0.

The estimator of F is based on the inversion formula for the Mellin transform. Some versions of this formula are known in the literature, see, e.g., Section 7 from [11], but here we need a slightly different form.

Lemma 2.1. *Let $\varphi : \mathbb{R}_+ \rightarrow \mathbb{R}$ be a non-decreasing function. Then*

1. *if there exists some $u^\circ \in (-\infty, 1) \cap \mathcal{C}_\varphi$, then $\varphi(0) < \infty$ and*

$$\frac{1}{2\pi i} \int_{u^\circ - i\infty}^{u^\circ + i\infty} x^{-z+1} \frac{\mathcal{M}[\varphi](z)}{-(z-1)} dz = \frac{1}{2} (\varphi(x+0) + \varphi(x-0)) - \varphi(0);$$

2. *if there exists some $u^\circ \in (1, \infty) \cap \mathcal{C}_\varphi$, then $\varphi(\infty) < \infty$ and*

$$\frac{1}{2\pi i} \int_{u^\circ - i\infty}^{u^\circ + i\infty} x^{-z+1} \frac{\mathcal{M}[\varphi](z)}{-(z-1)} dz = \frac{1}{2} (\varphi(x+0) + \varphi(x-0)) - \varphi(\infty).$$

Proof. The proof is given in Appendix B.1. \square

Remark 2.2. In what follows, for any non-decreasing function $\varphi : \mathbb{R}_+ \rightarrow \mathbb{R}$, we will use the same notation $\varphi(x)$, $x \in \mathbb{R}_+$, for the standardised version of the function, that is, for $(\varphi(x+0) + \varphi(x-0))/2$.

Motivated by Lemma 2.1, we define the estimator $\widehat{F}(x)$ of $F(x)$ as

$$\widehat{F}(x) := \frac{1}{2\pi} \int_{-\infty}^{\infty} x^{-u^\circ - iv + 1} \frac{\widehat{\mathcal{M}[F]}(u^\circ + iv)}{-(u^\circ + iv - 1)} K(v) dv \quad (4)$$

for some $u^\circ \in (-\infty, 1) \cap \mathcal{C}_F \cap \mathcal{H}_G$, and the kernel function K of the form

$$K(x) := \left(1 - \frac{|x|}{T}\right) \mathbb{I}\{|x| \leq T\}, \quad (5)$$

with a positive number T . This choice of the kernel function is inspired by the Berry – Esseen inequality for the Mellin transforms. In the next section, we discuss this inequality.

3 Berry – Esseen inequality for the Mellin transforms

The following lemma is motivated by a similar result for the Fourier transform, see Section 4.1 from [12].

Lemma 3.1. *Let $\varphi, \psi : \mathbb{R}_+ \rightarrow \mathbb{R}$ be two non-decreasing left continuous functions such that $\varphi(0) = \psi(0) = 0$. Let $u^\circ \in (-\infty, 1) \cap \mathcal{C}_\varphi \cap \mathcal{C}_\psi$. Denote*

$$\rho_{u^\circ}(\varphi, \psi) := \sup_{x \geq 0} |x^{u^\circ - 1}(\varphi(x) - \psi(x))|.$$

Assume that the supremum in the definition of $\rho_{u^\circ}(\varphi, \psi)$ is attained at some point $x_0 > 0$. Then for any $b > 2/\pi$, it holds

$$\begin{aligned} \rho_{u^\circ}(\varphi, \psi) &\leq \frac{b}{2} \int_{-T}^T \frac{|\mathcal{M}[\varphi](u^\circ + iv) - \mathcal{M}[\psi](u^\circ + iv)|}{|v|} dv \\ &\quad + bT x_0^{u^\circ - 1} \int_0^{2c(b)/T} |\psi(x_0) - \psi(x_0 e^r)| dr, \end{aligned} \quad (6)$$

where $c(b)$ can be found as a unique root of the equation

$$\int_{|r| \leq c(b)} \frac{\sin^2 r}{\pi r^2} dr = \frac{2}{3} \left(1 + \frac{1}{\pi b}\right), \quad (7)$$

and T is an arbitrary positive number such that

$$T > 2c(b)(1 - u^\circ)/\log 2. \quad (8)$$

Proof. The proof is given in Appendix B.2. \square

Remark 3.2. Since the left-hand side of the equation (7) tends to one as $c(b) \rightarrow \infty$, and to zero as $c(b) \rightarrow 0$, it can take any values from the interval $(0, 1)$. This is the reason for the restriction $b > 2/\pi$.

Remark 3.3. It is worth mentioning that the second term in the upper bound (6) tends to zero as $T \rightarrow \infty$ at a polynomial rate in the case when ψ is uniformly α -Hölder continuous with $\alpha \in (0, 1]$.¹ Indeed, we have

$$\int_0^{2c(b)/T} |\psi(x_0) - \psi(x_0 e^r)| dr \leq L_\psi x_0^\alpha \int_0^{2c(b)/T} |1 - e^r|^\alpha dr$$

for some $L_\psi \in (0, \infty)$. Using the inequality $e^x - 1 \leq x e^x$ which holds for any $x > 0$, we get

$$\int_0^{2c(b)/T} |1 - e^r|^\alpha dr \leq e^{2\alpha c(b)/T} \frac{(2c(b))^{1+\alpha}}{(1+\alpha)T^{1+\alpha}}.$$

Hence,

$$b T x_0^{u^\circ - 1} \int_0^{2c(b)/T} |\psi(x_0) - \psi(x_0 e^r)| dr \leq L_\psi x_0^{\alpha + u^\circ - 1} e^{2\alpha c(b)/T} \frac{b(2c(b))^{1+\alpha}}{(1+\alpha)T^\alpha},$$

yielding the polynomial rate of decay.

The numerical example of the use of the Berry – Esseen inequality is given in Appendix A.

4 Main results

In this section, we provide the rates of convergence of the estimate (4) with the kernel (5). The following theorem holds.

Theorem 4.1. *Let $u^\circ \in (-\infty, 1) \cap \mathcal{C}_F \cap \mathcal{H}_G$. Assume that the distribution function F is continuous at least in a small vicinity of 0, and*

$$x^{u^\circ - 1} F(x) \rightarrow 0 \quad \text{as } x \rightarrow 0. \quad (9)$$

Let $b > 2/\pi$ be an arbitrary number, $c(b)$ be the solution of the equation (7) and T satisfy (8). Then there exists some $x_0 > 0$ not depending on T and n

¹The asymptotic behaviour of the first term in (6) will be discussed later. Definitely, it depends on the closeness between the functions φ and ψ .

such that for any fixed $x > 0$, it holds with probability 1

$$\begin{aligned} \mathcal{R}(\hat{F}; u^\circ, x) &\leq \frac{b}{2T} \int_{-T}^T |\mathcal{M}[F](u^\circ + iv)| dv \\ &\quad + bT x_0^{u^\circ-1} \int_0^{2c(b)/T} |F(x_0) - F(x_0 e^r)| dr \\ &\quad + \frac{x^{u^\circ-1}}{2\pi n} \left| \sum_{k=1}^n \Lambda(X_k, x) \right|, \end{aligned}$$

where

$$\Lambda(X_k, x) = \int_{-\infty}^{\infty} x^{-(u^\circ-1)-iv} \frac{\mathcal{M}[F_{\text{mix}}](u^\circ + iv) - X_k^{(u^\circ-1)+iv}}{-(u^\circ + iv - 1) \mathcal{M}[G](u^\circ + iv)} K(v) dv.$$

Proof. The proof is given in Appendix B.3. \square

The preceding theorem allows us to further analyze the convergence of the estimator \hat{F} to the true c.d.f. F in the \mathcal{L}^2 -sense.

Theorem 4.2. *Under the same notations and assumptions as in Theorem 4.1, we get for any fixed $x > 0$,*

$$\begin{aligned} \mathcal{R}^*(\hat{F}; u^\circ, x) &\leq \frac{3b^2}{4T^2} \left(\int_{-T}^T |\mathcal{M}[F](u^\circ + iv)| dv \right)^2 \\ &\quad + 3b^2 T^2 x_0^{2(u^\circ-1)} \left(\int_0^{2c(b)/T} |F(x_0) - F(x_0 e^r)| dr \right)^2 \\ &\quad + \frac{3x^{2(u^\circ-1)}}{4\pi^2 n} \int_{-T}^T \frac{1}{((u^\circ - 1)^2 + v^2) |\mathcal{M}[G](u^\circ + iv)|^2} dv \\ &\quad \times \int_{\mathbb{R}} |\mathcal{M}[F_{\text{mix}}](2u^\circ - 1 + iw)| dw. \quad (10) \end{aligned}$$

Proof. The proof is given in Appendix B.4. \square

5 Convergence rates

Denote the summands in (10) by I_1, I_2, I_3 , respectively. Let us consider these summands separately.

1. Let us first note that the condition

$$\int_{\mathbb{R}} |\mathcal{M}[F](u^\circ + iv)| dv < \infty \quad (11)$$

is fulfilled for many distributions, including the distributions with exponential and polynomial decay of the Mellin transform, see [4]. The condition (11) yields that **the first summand** is of order $I_1 = O(T^{-2})$ as $T \rightarrow \infty$. Nevertheless, it can be shown that any distribution satisfying (11) is absolutely continuous. This fact can be proved in various ways, e.g., via the convergence in $\mathcal{L}^2(\mathbb{R})$, along the same lines as the proof of the similar fact for the Fourier transform, see Lemma 1.1 from [10]. It can be also derived from the properties of the Fourier transform (see Theorem 3.2.2 from [13]). In fact,

$$\begin{aligned} \int_{\mathbb{R}} |\mathcal{M}[F](u^\circ + iv)| dv &= \int_{\mathbb{R}} \left| \int_{\mathbb{R}^+} x^{u^\circ + iv - 1} dF(x) \right| dv \\ &= \int_{\mathbb{R}} \left| \int_{\mathbb{R}} e^{iyv} \cdot e^{y(u^\circ - 1)} dF(e^y) \right| dv \\ &= \mathcal{M}[F](u^\circ) \int_{\mathbb{R}} \left| \int_{\mathbb{R}} e^{iyv} dH(y) \right| dv, \end{aligned}$$

where

$$\begin{aligned} H(y) &:= \frac{1}{\mathcal{M}[F](u^\circ)} \int_{-\infty}^y e^{s(u^\circ - 1)} dF(e^s) \\ &= \frac{1}{\mathcal{M}[F](u^\circ)} \int_0^{e^y} x^{u^\circ - 1} dF(x), \quad y \in \mathbb{R}, \end{aligned}$$

is a distribution function (here we use that $\mathcal{M}[F](u^\circ) < \infty$ since $u^\circ \in \mathcal{C}_F$). Therefore, the condition (11) is equivalent to $\mathcal{F}[H] \in \mathcal{L}^1(\mathbb{R})$, which yields that the H is a c.d.f. of an absolutely continuous distribution with bounded and continuous density function. Then the distribution of F is absolutely continuous as well.

2. The typical order for **the second summand** is also $O(T^{-2})$. In fact, if F is Lipschitz continuous, we get from Remark 3.3

$$I_2 \leq L_F^2 x_0^{2u^\circ} e^{4c(b)/T} \frac{12b^2(c(b))^4}{T^2}$$

where $L_F \in (0, \infty)$ is the Lipschitz constant of F .

3. To establish the asymptotic order of **the third summand** I_3 , we observe that, since $u^\circ \in \mathcal{H}_G \subset \mathcal{C}_G$, for any $T > 0$, there exist positive constants $C_{u^\circ, T}^{(1)}, C_{u^\circ, T}^{(2)}$ such that

$$C_{u^\circ, T}^{(1)} \leq |\mathcal{M}[G](u^\circ + iv)| \leq C_{u^\circ, T}^{(2)}, \quad \forall v \in [-T, T]. \quad (12)$$

Assuming that $2u^\circ - 1 \in \mathcal{H}_G$, we similarly get with some positive constants $C_{2u^\circ-1,T}^{(1)}, C_{2u^\circ-1,T}^{(2)}$

$$C_{2u^\circ-1,T}^{(1)} \leq |\mathcal{M}[G](u^\circ + iv)| \leq C_{2u^\circ-1,T}^{(2)}, \quad \forall v \in [-T, T]. \quad (13)$$

Let us assume additionally that as $T \rightarrow \infty$,

$$C_{u^\circ,T}^{(1)} \rightarrow C_{u^\circ}^{(1)} > 0 \quad \text{and} \quad C_{2u^\circ-1,T}^{(2)} \rightarrow C_{2u^\circ-1}^{(2)} < \infty.$$

We refer to Section 6 for examples of mixing distributions which satisfy this assumption. Finally, assume that the analogue of (11) holds along the line $\text{Re}(z) = 2u^\circ - 1$,

$$\int_{\mathbb{R}} |\mathcal{M}[F](2u^\circ - 1 + iv)| dv \leq C_1 < \infty. \quad (14)$$

Then we get

$$I_3 \leq \frac{3x^{2(u^\circ-1)}}{4\pi^2 n} \frac{C_1 C_{2u^\circ-1}^{(2)}}{\left(C_{u^\circ}^{(1)}\right)^2} \int_{-T}^T \frac{1}{(u^\circ - 1)^2 + v^2} dv = \frac{3x^{2(u^\circ-1)} C_1 C_{2u^\circ-1}^{(2)}}{4(1 - u^\circ) \pi \left(C_{u^\circ}^{(1)}\right)^2 n}.$$

provided that (11) holds. Finally, let us note that the choice $T = O(n^{1/2})$ leads to the rate of convergence $I_1 + I_2 + I_3 = O(1/n)$ which coincides with the rate in the case when the direct observations from F are available.

6 The set \mathcal{H}_G

The set \mathcal{H}_G defined by (3) plays a crucial role in the analysis. Let us show that this set is nonempty for positive discrete distributions separated from 0. Indeed, consider a random variable η taking K positive values $\sigma_1, \dots, \sigma_K$ with probabilities $p_1, \dots, p_K > 0$, $\sum_{k=1}^K p_k = 1$ (the analysis of the case $K = \infty$ follows the same lines). Without loss of generality, assume that $0 < \sigma_1 < \sigma_2 < \dots < \sigma_K$. Then it holds

$$\mathcal{M}[G](u + iv) = \sum_{k=1}^K \sigma_k^{u+iv-1} p_k = \sigma_1^{u+iv-1} p_1 + \sum_{k=2}^K \sigma_k^{u+iv-1} p_k, \quad (15)$$

where the modulus of the second summand can be upper bounded as

$$\left| \sum_{k=2}^K \sigma_k^{u+iv-1} p_k \right| \leq \sum_{k=2}^K |\sigma_k^{u+iv-1}| p_k = \sum_{k=2}^K \sigma_k^{u-1} p_k < \sigma_2^{u-1} (1 - p_1)$$

for any $u < 1$, while the modulus of the first summand in (15) is equal to $\sigma_1^{u-1} p_1$. From this it follows that

$$|M[G](u + iv)| \geq |\sigma_1^{u+iv-1} p_1| - \left| \sum_{k=2}^K \sigma_k^{u+iv-1} p_k \right| > \sigma_1^{u-1} p_1 - \sigma_2^{u-1} (1 - p_1),$$

where the expression on the right-hand side is strongly positive for any

$$u < \frac{\log(p_1/(1 - p_1))}{\log(\sigma_2/\sigma_1)} + 1. \quad (16)$$

Let us provide a couple of examples.

1. Consider the geometric distribution defined as a distribution of a r.v. η such that

$$\mathbb{P}\{\eta = k\} = pq^{k-1}, \quad k = 1, 2, \dots$$

According to (16), the absolute value of the Mellin transform of this distribution is strongly positive for any

$$u < \frac{\log(p/(1 - p))}{\log(2)} + 1,$$

where the expression on the r.h.s. is positive for $p > 1/3$ and negative for $p < 1/3$.

2. Consider an analogue of the Poisson distribution on $\{1, 2, \dots\}$:

$$\mathbb{P}\{\eta = k\} = \frac{e^{-\lambda}}{1 - e^{-\lambda}} \cdot \frac{\lambda^k}{k!}, \quad k = 1, 2, 3, \dots,$$

where $\lambda > 0$. Returning to (16), we get that the absolute value of the Mellin transform is strongly positive in absolute value for any

$$u < \frac{\log(\lambda e^{-\lambda}/(1 - e^{-\lambda} - \lambda e^{-\lambda}))}{\log(2)} + 1,$$

which is positive whenever $\lambda \in (0, \lambda_0)$ with λ_0 defined as the positive solution of the equation $3\lambda + 1 = e^\lambda$. Numerically we get $\lambda_0 \approx 1.9$.

Note that in some simple cases the result can be enhanced.

1. For instance, consider the zeta distribution

$$\mathbb{P}\{\eta = k\} = \frac{1}{\zeta(s)} k^{-s}, \quad k = 1, 2, \dots, \quad (17)$$

where $s > 1$ and $\zeta(s)$ is the Riemann zeta function defined as

$$\zeta(s) = \sum_{k=1}^{\infty} k^{-s}.$$

Since $\mathcal{M}[G](u+iv) = \zeta(1+s-u-iv)/\zeta(s)$, and the zeta-function has no zeros with real part larger than 1, we get that the set \mathcal{H}_G contains all $u < s$.

2. Consider the distribution of the random variable taking values $\sigma_1 = 1$ and $\sigma_2 > 1$ with probabilities $p \in (0, 1)$ and $1-p$. Then any

$$u \neq u_{\circ} := 1 + \log_{\sigma_2}(p/(1-p)) \quad (18)$$

belong to the set \mathcal{H}_G . In fact, in this case the Mellin transform can be lower bounded for any $v \in \mathbb{R}$ by

$$|\mathcal{M}[G](u+iv)| \geq |p - (1-p)\sigma_2^{u-1}|,$$

which is strongly larger than 0 for any $u \neq u_{\circ}$.

7 Numerical examples

In this section we use simulated data to illustrate the behaviour of the proposed estimator for different types of mixing distributions G . We also compare our estimator with another one based on a logarithmic transformation of both sides in (1) and interpretation of the problem as an additive deconvolution problem. Since $\phi_{\log X}(t) = \phi_{\log Y}(t)\phi_{\log \eta}(t)$, $\forall t \in \mathbb{R}$ where ϕ denotes a characteristic function, the inversion formula for the Fourier-Stieltjes transform (see Theorem 4.4.1 in Kawata, 1972) suggests that F can be estimated using

$$\widehat{F}_{\log Y}(x) - \widehat{F}_{\log Y}(0) = \frac{1}{2\pi} \int_{-R_n}^{R_n} \frac{e^{-itx} - 1}{-it} \cdot \frac{\widehat{\phi}_{\log X}(t)}{\widehat{\phi}_{\log \eta}(t)} \phi_{\kappa}(ht) dt, \quad (19)$$

where $\widehat{\phi}_{\log X}(t) = \frac{1}{n} \sum_{j=1}^n e^{it \log X_j}$, $R_n \rightarrow \infty$ as $n \rightarrow \infty$, h is a bandwidth parameter chosen by the cross-validation approach, and ϕ_{κ} is the characteristic function of some kernel function κ which we choose to be density of the standard normal law; for details see, e.g., Delaigle (2021).

In what follows, we assume that the unknown distribution F is absolutely continuous. More precisely, consider the cases when F is a c.d.f. of the beta distribution

$$F(x) = \frac{\mathbb{I}\{x \in [0, 1]\}}{B(\alpha_1, \alpha_2)} \int_0^x y^{\alpha_1-1} (1-y)^{\alpha_2-1} dy + \mathbb{I}\{x > 1\}$$

and the gamma distribution

$$F(x) = \frac{\theta^k}{\Gamma(k)} \int_0^x y^{k-1} e^{-\theta y} dy \cdot \mathbb{I}\{x > 0\}$$

with parameters $\alpha_1 = \alpha_2 = k = \theta = 2$. Note that $\mathcal{C}_F = (1 - \alpha_1, \infty)$ for the beta distribution and $\mathcal{C}_F = (1 - k, \infty)$ for the gamma distribution. Also note that the assumption (9) holds for both examples: in fact, since $F(0) = 0$, we get by the L'Hôpital rule

$$\lim_{x \rightarrow 0} x^{u^\circ - 1} F(x) = \frac{1}{1 - u^\circ} \lim_{x \rightarrow 0} x^{u^\circ} F'(x),$$

where the limit on the right-hand side is finite for any $u^\circ \in (1 - \alpha_1, 1) = (-1, 1)$ in the case of the beta distribution, and for any $u^\circ \in (1 - k, 1) = (-1, 1)$ in the case of the gamma distribution. In what follows, we consider the estimate (4) with the kernel (5).

1. Discrete mixing distribution with finite support. Let G be a purely discrete probability law taking values 1 and 2 with probabilities 1/3 and 2/3, respectively. As was discussed in Section 6, we have in this case

$$|\mathcal{M}[G](u + iv)| \neq 0 \quad \text{for any } u \neq 1 + \log_2 \frac{1/3}{2/3} = 0 \quad \text{and any } v \in \mathbb{R}.$$

Therefore the parameter u° can be taken from the set

$$(-\infty, 1) \cap \mathcal{C}_F \cap \mathcal{H}_G = (-1, 0) \cup (0, 1).$$

In what follows, we take $u^\circ = 1/2$. Based on the discussion in Section 5, we choose $T_n = n = 1000$. As for the estimator (19), the parameter R_n minimises the corresponding mean-square error based on 500 samples of size $n = 1000$. The exact values are 3.5 and 9.7 for the beta and the gamma distributions, respectively.

Figure 1 shows boxplots of the mean-squared errors of the Mellin-based estimator (4) and the Fourier-based estimator (19) for different values of $n \in \{100, 500, 1000\}$ obtained via 100 simulation runs. The average (over runs) values of MSE for each n are presented in Table 1. Note that for both beta and gamma distributions the proposed estimator (4) converges to the true c.d.f. F rather fast with the MSE being less than 0.003 for $n = 1000$. To the contrary, the accuracy of the estimator (19) does not significantly increase with the growth of n , and the average errors are more than 60 times greater than those of the estimator (4). This point is also justified by Figures 2 and 3 showing the estimated

Table 1: Average MSE for the Mellin-based estimator (4) and the Fourier-based estimator (19) obtained via 100 simulation runs

		Beta(2,2) distribution		
Mixing distribution		Method		Relative error
		Mellin	Fourier	Fourier/Mellin
Two point	$n = 100$	0.0012	0.2128	177.33
	$n = 500$	0.0003	0.2093	697.67
	$n = 1000$	0.0002	0.2092	1046
Zeta	$n = 100$	0.000069	0.00011	1.59
	$n = 500$	0.000074	0.00011	1.49
	$n = 1000$	0.000068	0.0001	1.47
Uniform	$n = 100$	0.0051	0.0046	0.9
	$n = 500$	0.0014	0.0012	0.86
	$n = 1000$	0.00071	0.00072	1.01

		Gamma(2,2) distribution		
Mixing distribution		Method		Relative error
		Mellin	Fourier	Fourier/Mellin
Two point	$n = 100$	0.0012	0.0728	60.67
	$n = 500$	0.0003	0.0723	241
	$n = 1000$	0.0001	0.0716	716
Zeta	$n = 100$	0.0008	0.0022	2.75
	$n = 500$	0.0002	0.0004	2
	$n = 1000$	0.00008	0.0002	2.5
Uniform	$n = 100$	0.004	0.0035	0.88
	$n = 500$	0.001	0.0007	0.7
	$n = 1000$	0.0006	0.0004	0.67

and true c.d.f.s.

Figure 4 represents the dependence of the left-hand side in Theorem 4.1 on x (with fixed $u = 0.5$) and u° (with fixed $x = 0.5$) for 25 samples of size $n = 1000$. The plots indicate that for both beta and gamma distributions the accuracy of the estimator increases with growing x which is coherent with the theoretical findings of Theorem 4.1. As for dependence on u° , one can observe that, as suggested by Theorem 4.1, the proposed estimator becomes more accurate as u° increases with an evident exception for $u^\circ = 0$. As was mentioned earlier in this section, the reason for this peculiarity is that $u^\circ = 0$ turns out to be exactly the threshold value (18), for which the Mellin transform $\mathcal{M}[G](z)$ of the mixing distribution is not guaranteed to be separated from zero in absolute value.

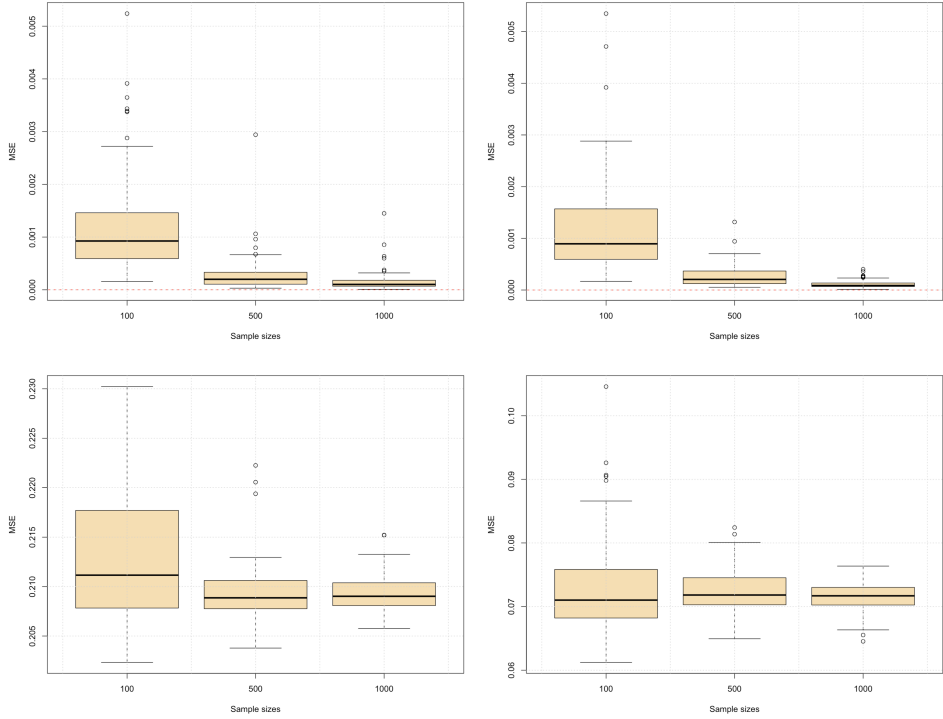


Figure 1: The mean-squared errors of the estimators (4) (top) and (19) (bottom) for the c.d.f.s of Beta(2,2) (left) and Gamma(2,2) (right) distributions based on 100 simulation runs for G being a c.d.f. of a discrete distribution supported on two points.

2. Discrete mixing distribution with infinite support. Now let G be the c.d.f. of the zeta distribution (17) with parameter $s = 5$. As was discussed in Section 6, in this case $|\mathcal{M}[G](u^\circ + iv)|$ is strictly positive for any

$$u^\circ < -\frac{\log(\zeta(5))}{\log(2)} + 1 \approx 0.95.$$

Figure 5 shows the mean-square errors of the estimators (4) and (19). As before, the parameters for (4) are fixed as $T_n = 1000$ and $u^\circ = 0.5$. The cutoff parameter R_n for the estimator (19) was chosen by the same methodology as before resulting in the values 9.6 for beta distribution and 45.4 for gamma law. It can be observed that in case of the latter the errors for both estimators converge to zero as n grows. However, the proposed estimator outperforms the one based on the Fourier transform as follows from the average errors depicted in Table 1. In case of beta distribution, the average errors for both estimators are

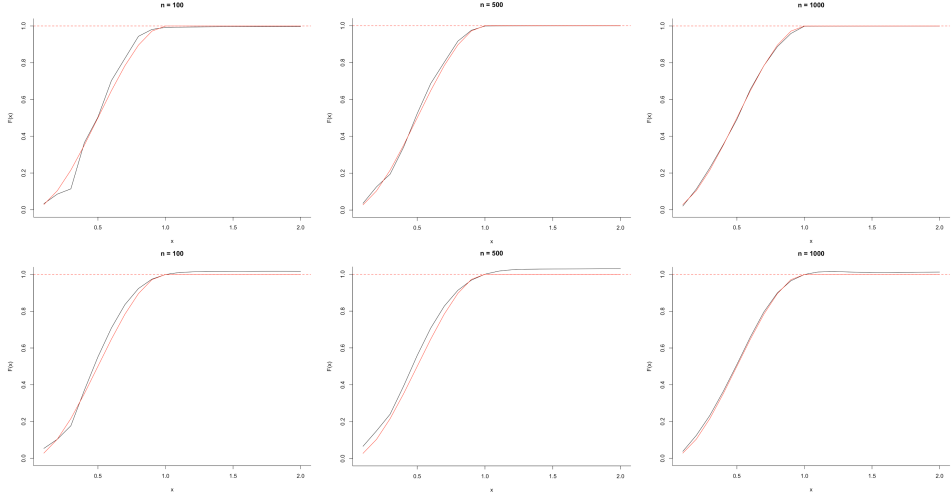


Figure 2: The estimates \hat{F} of the c.d.f. of the Beta(2,2) distribution for the estimators (4) based on the Mellin transform (top) and (19) based on the Fourier transform (bottom) superimposed with the true distribution function for G being a c.d.f. of a discrete distribution supported on two points.

smaller than 0.0009 already for $n = 100$, and further convergence to zero appears to be very slow. Nevertheless, the estimator (4) still has slightly smaller errors and yields a more accurate fit compared to (19), as follows from Figures 6 and 7.

Figure 8 illustrates the dependence of the estimated left-hand side in Theorem 4.1 on x and u° for 25 samples of size $n = 1000$. As before, in the first case the parameter u° was fixed as $u^\circ = 0.5$. It can be observed that for both beta and gamma distributions the accuracy of the proposed estimator increases as x grows, though for the former the dependence is more unstable. In case of dependence on u° , the parameter x was fixed at the same level $x = 0.5$. From the plots on the right of Figure 8 one can observe that the error strictly decreases with growing u° . Hence, the estimator becomes more accurate as x and u° increase, which supports the theoretical findings of Theorem 4.1.

3. Continuous mixing distribution. Finally, assume that G corresponds to the c.d.f. of the uniform distribution on $[0, 1]$. In this case, we have

$$|\mathcal{M}[G](u^\circ + iv)| = |u^\circ + iv|^{-1} > 0$$

for any $u^\circ, v \in \mathbb{R}$. However, since $|\mathcal{M}[G](u^\circ + iv)|$ decreases in v and can become arbitrarily close to zero as $|v| \rightarrow \infty$, the choice of the

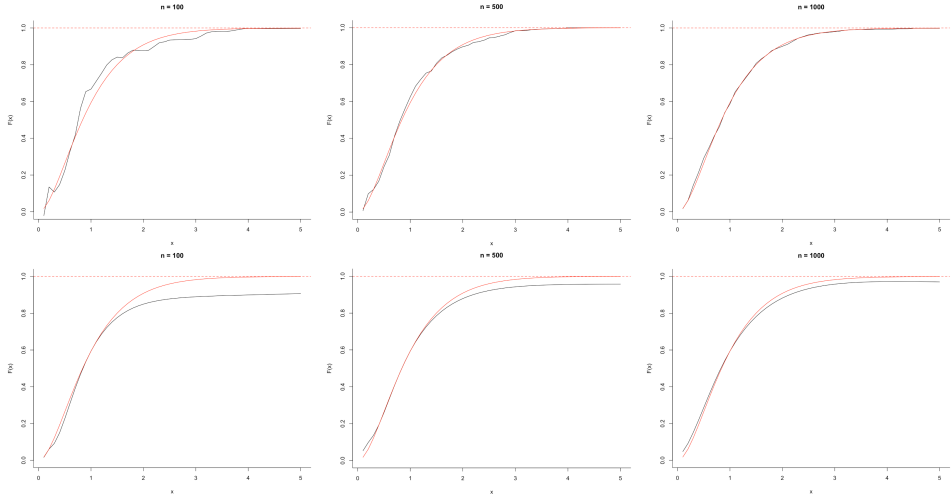


Figure 3: The estimates \hat{F} of the c.d.f. of the $\text{Gamma}(2,2)$ distribution for the estimators (4) based on the Mellin transform (top) and (19) based on the Fourier transform (bottom) superimposed with the true distribution function for G being a c.d.f. of a discrete distribution supported on two points

truncation level T_n for (4) becomes crucial. In what follows, we use the values $T_n = 34.6$ and $T_n = 29.7$ for the cases of beta and gamma distributions, respectively. These values were obtained by the same methodology as described above for the estimator (19). As for the latter, the values of R_n minimising the MSE turned out to be $R_n = 9.7$ for the beta distribution and $R_n = 3.4$ for the gamma law.

Figure 9 represents the mean-square errors for estimators (4) and (19). It can be observed that both methods provide very similar results, with the latter estimator performing a bit better in case of the gamma distribution. In both cases, the error decreases as the sample size grows, though the rate of convergence to zero appears to be slower than for discrete mixing distributions considered above. This observation is further supported by Figures 10 and 11 showing the fits provided by the above two estimators.

Finally, Figure 12 represents the boxplots of the estimated $\hat{\mathcal{R}}(\hat{F}; u^\circ, x)$ for the proposed estimator (4) for different values of x and u° . The parameters were fixed as $x = u^\circ = 0.5$, and the boxplots were obtained based on 25 samples of size $n = 1000$ as before. It can be seen that the accuracy of the estimator increases with growing x and u° .

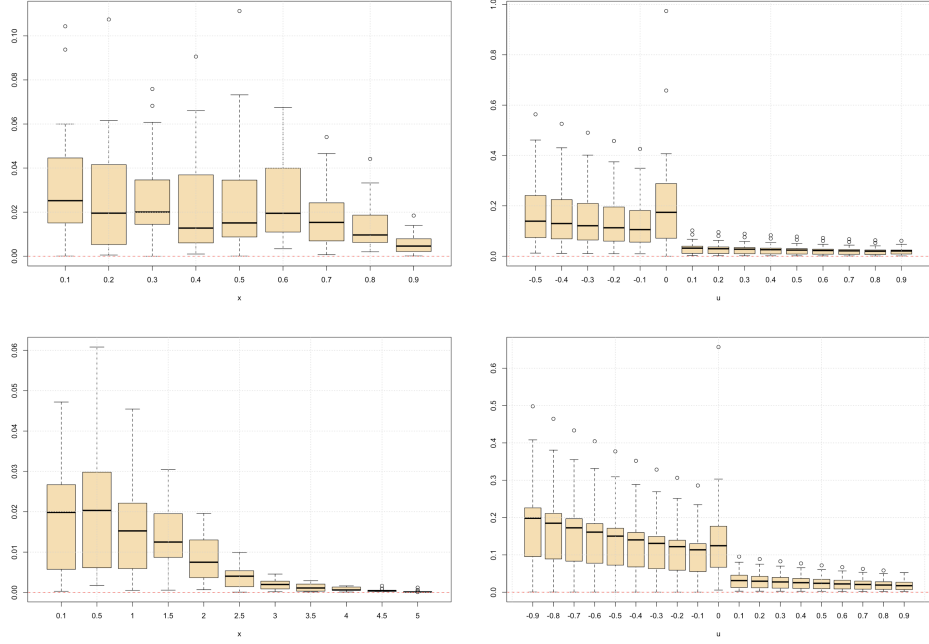


Figure 4: The estimates $\widehat{\mathcal{R}}(\widehat{F}; u^\circ, x)$ for different values of x (left) and u° (right) for Beta(2,2) (top) and Gamma(2,2) (bottom) distributions for G being a c.d.f. of a discrete distribution supported on two points

A Berry – Esseen inequality in a particular case

Let us consider the case when φ and ψ are the distribution functions of the exponential distribution, that is,

$$\varphi(x) = (1 - e^{-\lambda_1 x}) \mathbb{I}\{x \geq 0\}, \quad \psi(x) = (1 - e^{-\lambda_2 x}) \mathbb{I}\{x \geq 0\},$$

where $\lambda_1, \lambda_2 > 0$. Since

$$\mathcal{M}[\varphi](z) = \lambda_1^{1-z} \Gamma(z), \quad \mathcal{M}[\psi](z) = \lambda_2^{1-z} \Gamma(z)$$

for any z with $\text{Re}(z) > 0$, we can take $u^\circ = 1/2$. We have

$$\rho_{1/2}(\varphi, \psi) := \sup_{x \geq 0} \left| \frac{e^{-\lambda_1 x} - e^{-\lambda_2 x}}{\sqrt{x}} \right|.$$

The maximum is attained at some point $x_0 \in (0, \infty)$. For this numerical example we take the values $\lambda_1 = 1, \lambda_2 = 1.5$, for which $x_0 = 0.4$.

We also take $b = 0.8$, and numerically get $c(0.8) \approx 4.8$ as the solution of (7). We aim to study the right-hand side of (6) depending on T .

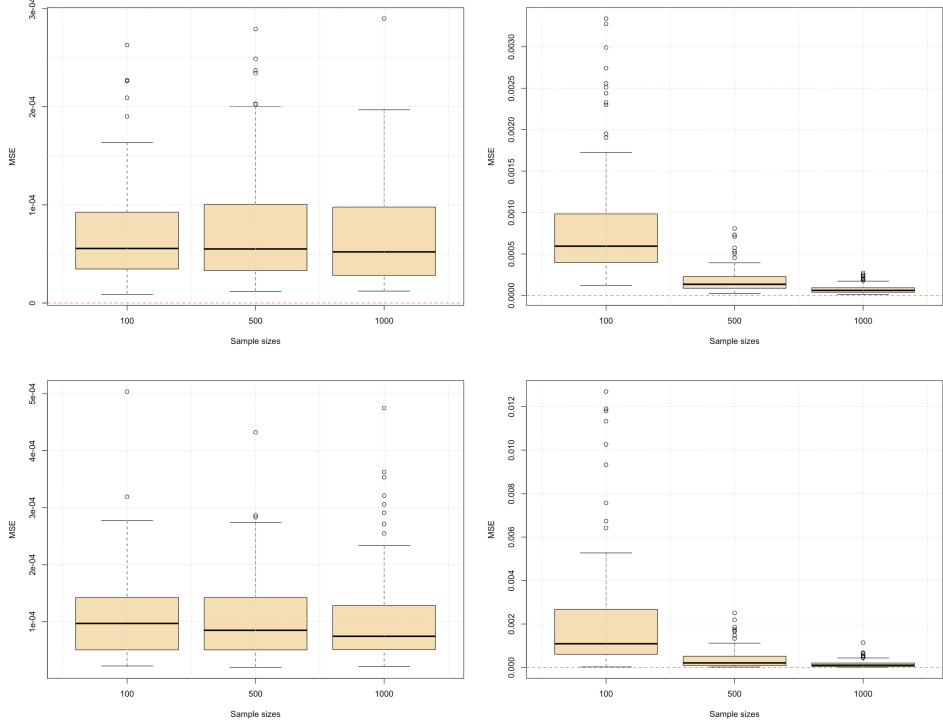


Figure 5: The mean-squared errors of the estimators (4) (top) and (19) (bottom) for the c.d.f.s of Beta(2,2) (left) and Gamma(2,2) (right) distributions based on 100 simulation runs for G being a c.d.f. of the zeta distribution

Figure 13 represents the plots of the first and the second summands in (6), namely,

$$\begin{aligned}
 I_1 &= \frac{b}{2} \int_{-T}^T \frac{|\lambda_1^{1/2-iv} - \lambda_2^{1/2-iv}|}{|v|} |\Gamma((1/2) + iv)| dv, \\
 I_2 &= b T x_0^{u^\circ - 1} \int_0^{2c(b)/T} (e^{x_0 e^r} - e^{x_0}) dr.
 \end{aligned}$$

An interesting observation is that I_1 is almost equal to a constant for large T , while I_2 decays rather fast as T grows.

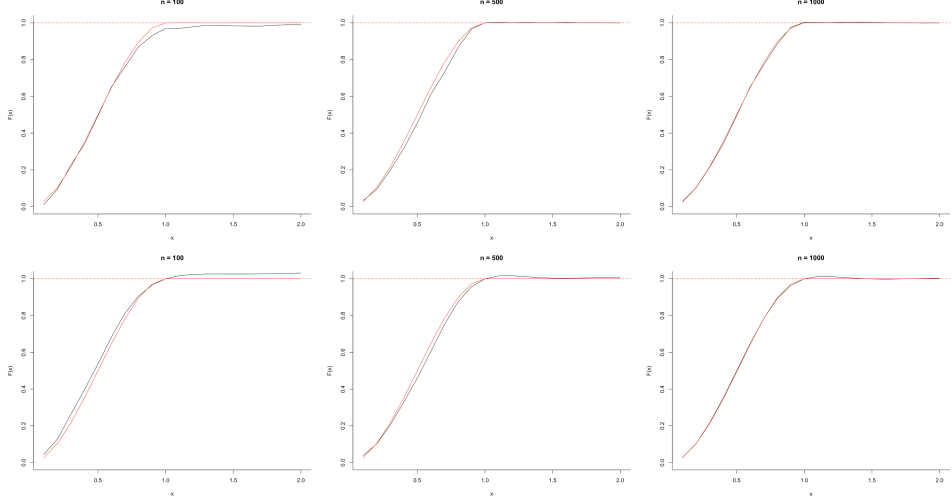


Figure 6: The estimates \hat{F} of the c.d.f. of the Beta(2,2) distribution for the estimators (4) based on the Mellin transform (top) and (19) based on the Fourier transform (bottom) superimposed with the true distribution function for G being a c.d.f. of the zeta distribution

B Proofs

B.1 Proof of Lemma 2.1

Let us rewrite (2) as

$$\begin{aligned} \mathcal{M}[\varphi](z) &= \int_0^\infty x^{z-1} d\varphi(x) = \int_0^\infty e^{(z-1)\log x} d\varphi(e^{\log x}) \\ &= \int_{-\infty}^\infty e^{-sy} d\varphi(e^y) =: \mathcal{L}[\varphi(e^y)](s), \end{aligned}$$

where the right-hand side defines the bilateral Laplace transform of $\varphi(e^y)$, $y = \log x$, at the point $s = -(z - 1)$. Applying Theorem 7.7.5 from [11] for the bilateral Laplace transform, we arrive at

$$\begin{aligned} \frac{1}{2}(\varphi(e^y + 0) + \varphi(e^y - 0)) - \varphi(0) &= \frac{1}{2\pi i} \int_{\tilde{u}-i\infty}^{\tilde{u}+i\infty} e^{sy} \frac{\mathcal{L}[\varphi(e^y)](s)}{s} ds \\ &= \frac{1}{2\pi i} \int_{u^\circ-i\infty}^{u^\circ+i\infty} x^{-z+1} \frac{\mathcal{M}[\varphi](z)}{-(z-1)} dz, \end{aligned}$$

provided $\tilde{u} := 1 - u^\circ > 0$. The second statement of the theorem follows from another part of Theorem 7.7.5 from [11]

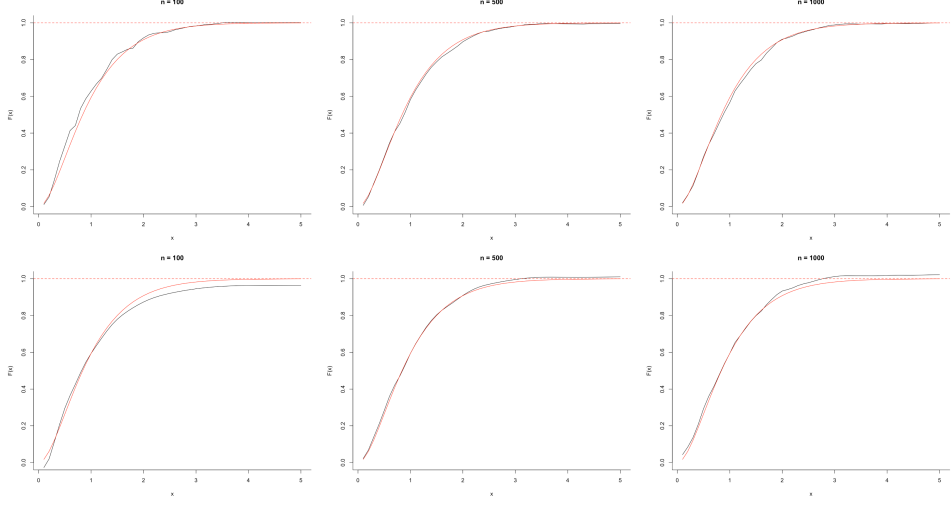


Figure 7: The estimates \widehat{F} of the c.d.f. of the $\text{Gamma}(2,2)$ distribution for the estimators (4) based on the Mellin transform (top) and (19) based on the Fourier transform (bottom) superimposed with the true distribution function for G being a c.d.f. of the zeta distribution

B.2 Proof of Lemma 3.1

Let

$$w(x) = \frac{\sin^2(T \log x)}{\pi T x^{u^\circ} \log^2 x} \quad \text{and} \quad W(x) = \int_0^x w(y) dy, x \in \mathbb{R}_+. \quad (20)$$

Define

$$\tilde{\varphi}(x) := \int_0^\infty \varphi(x/y) dW(y), \quad \tilde{\psi}(x) := \int_0^\infty \psi(x/y) dW(y).$$

Due to Theorem 7.8.3 from [11],

$$\mathcal{M}[\tilde{\varphi}](z) = \mathcal{M}[\varphi](z) \mathcal{M}[W](z), \quad \mathcal{M}[\tilde{\psi}](z) = \mathcal{M}[\psi](z) \mathcal{M}[W](z).$$

Then, by the inverse formula for the Mellin transform (Lemma 2.1),

$$\begin{aligned} \tilde{\varphi}(x) - \tilde{\psi}(x) &= \frac{1}{2\pi i} \int_{u^\circ - i\infty}^{u^\circ + i\infty} \frac{\mathcal{M}[\varphi](z) - \mathcal{M}[\psi](z)}{-(z-1)} \mathcal{M}[W](z) x^{-z+1} dz \\ &= \frac{1}{2\pi} \int_{-\infty}^\infty \frac{\mathcal{M}[\varphi](u^\circ + iv) - \mathcal{M}[\psi](u^\circ + iv)}{-(u^\circ + iv - 1)} \mathcal{M}[W](u^\circ + iv) x^{-u^\circ - iv + 1} dv. \end{aligned}$$

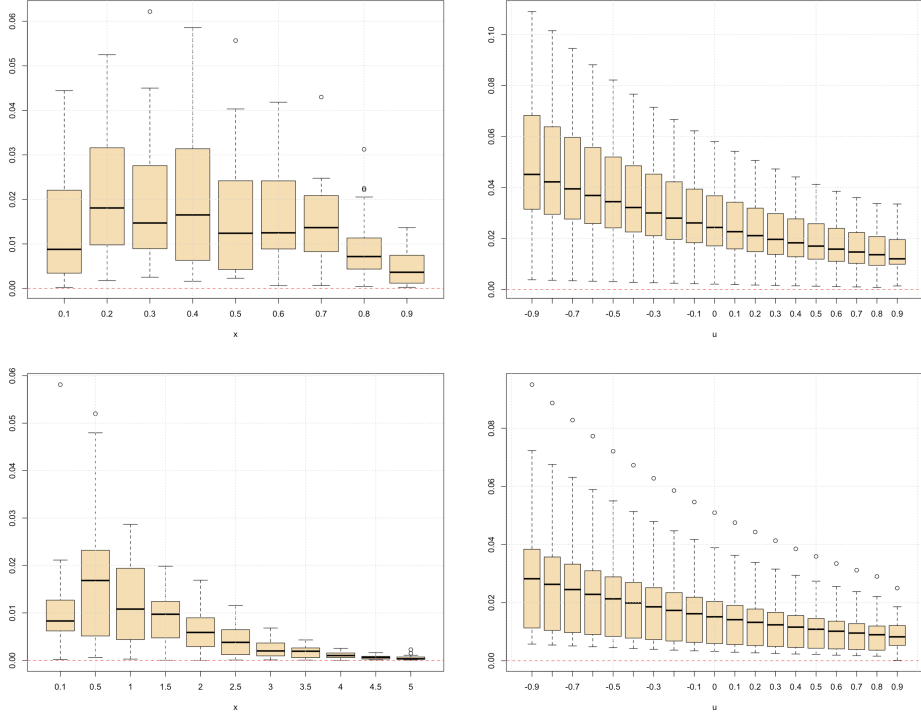


Figure 8: The estimates $\widehat{\mathcal{R}}(\widehat{F}; u^\circ, x)$ for different values of x (left) and u° (right) for Beta(2,2) (top) and Gamma(2,2) (bottom) distributions for G being a c.d.f. of the zeta distribution

We get

$$\begin{aligned}
 \mathcal{M}[W](u^\circ + iv) &= \int_0^\infty x^{(u^\circ-1)+iv} \frac{\sin^2(T \log x)}{\pi T x^{u^\circ} \log^2 x} dx \\
 &= \int_{-\infty}^\infty e^{ivy} \frac{\sin^2(Ty)}{\pi Ty^2} dy \\
 &= \left(1 - \left|\frac{v}{T}\right|\right) \mathbb{I}\{|v| \leq T\},
 \end{aligned} \tag{21}$$

hence,

$$\begin{aligned}
 \rho_{u^\circ}(\tilde{\varphi}, \tilde{\psi}) &\leq \frac{1}{2\pi} \int_{-T}^T \frac{|\mathcal{M}[\varphi](u^\circ + iv) - \mathcal{M}[\psi](u^\circ + iv)|}{\sqrt{(u^\circ - 1)^2 + v^2}} dv \\
 &\leq \frac{1}{2\pi} \int_{-T}^T \frac{|\mathcal{M}[\varphi](u^\circ + iv) - \mathcal{M}[\psi](u^\circ + iv)|}{|v|} dv.
 \end{aligned} \tag{22}$$

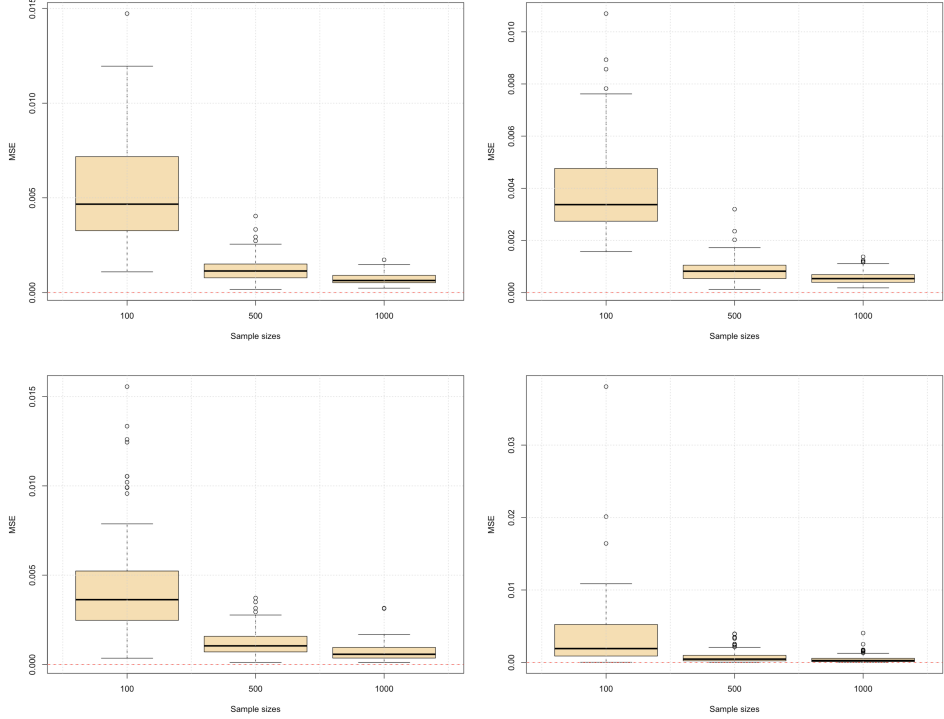


Figure 9: The mean-squared errors of the estimators (4) (top) and (19) (bottom) for the c.d.f.s of Beta(2,2) (left) and Gamma(2,2) (right) distributions based on 100 simulation runs for G being a c.d.f. of the uniform distribution

At the same time,

$$\begin{aligned}
 \tilde{\varphi}(x) - \tilde{\psi}(x) &= \int_0^\infty (\varphi(x/y) - \psi(x/y)) w(y) dy \\
 &= \int_0^\infty (\varphi(x/y) - \psi(x/y)) \frac{\sin^2(T \log y)}{\pi T y^{u^\circ} \log^2 y} dy.
 \end{aligned}$$

Let us denote $\Delta = \rho_{u^\circ}(\varphi, \psi)$. Then

$$x_0^{u^\circ-1}(\varphi(x_0) - \psi(x_0 \pm 0)) = \Delta$$

or

$$x_0^{u^\circ-1}(\psi(x_0 \pm 0) - \varphi(x_0 - 0)) = \Delta.$$

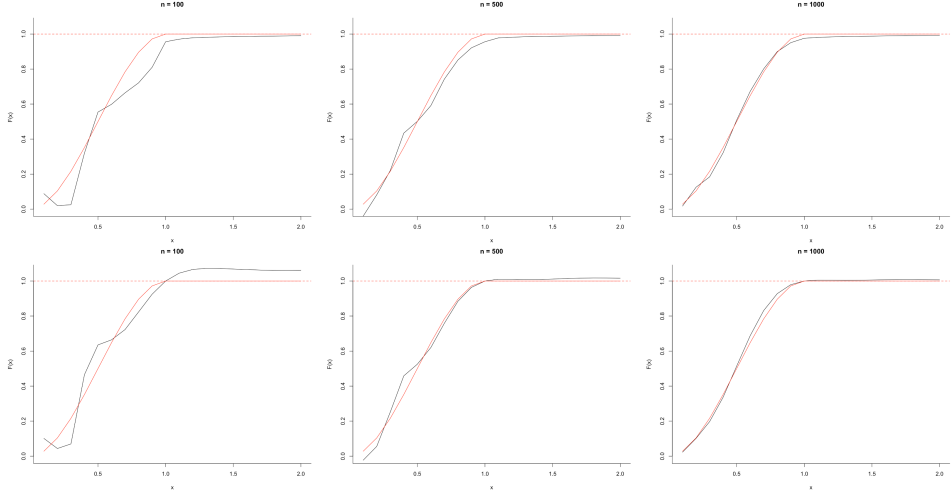


Figure 10: The estimates \hat{F} of the c.d.f. of the Beta(2,2) distribution for the estimators (4) based on the Mellin transform (top) and (19) based on the Fourier transform (bottom) superimposed with the true distribution function for G being a c.d.f. of the uniform distribution

Since for both cases the proof follows the same lines, we will only consider the first one. In this case

$$\begin{aligned}
& x_0^{u^\circ-1} e^{\frac{c(b)(u^\circ-1)}{T}} \left(\tilde{\varphi} \left(x_0 e^{\frac{c(b)}{T}} \right) - \tilde{\psi} \left(x_0 e^{\frac{c(b)}{T}} \right) \right) \\
&= x_0^{u^\circ-1} e^{\frac{c(b)(u^\circ-1)}{T}} \int_0^\infty \left(\varphi(x_0 e^{\frac{c(b)}{T}}/y) - \psi(x_0 e^{\frac{c(b)}{T}}/y) \right) \frac{\sin^2(T \log y)}{\pi T y^{u^\circ} \log^2 y} dy \\
&= x_0^{u^\circ-1} \int_{-\infty}^\infty \left(\varphi(x_0 e^{\frac{c(b)-r}{T}}) - \psi(x_0 e^{\frac{c(b)-r}{T}}) \right) \frac{\sin^2 r}{\pi r^2} e^{(c(b)-r)(u^\circ-1)/T} dr \\
&= x_0^{u^\circ-1} \int_{|r|<c(b)} \left(\varphi(x_0 e^{\frac{c(b)-r}{T}}) - \psi(x_0 e^{\frac{c(b)-r}{T}}) \right) \frac{\sin^2 r}{\pi r^2} e^{(c(b)-r)(u^\circ-1)/T} dr \\
&\quad + x_0^{u^\circ-1} \int_{|r|\geq c(b)} \left(\varphi(x_0 e^{\frac{c(b)-r}{T}}) - \psi(x_0 e^{\frac{c(b)-r}{T}}) \right) \frac{\sin^2 r}{\pi r^2} e^{(c(b)-r)(u^\circ-1)/T} dr \\
&\geq x_0^{u^\circ-1} \int_{|r|<c(b)} \left(\psi(x_0 \pm 0) - \psi(x_0 e^{\frac{c(b)-r}{T}}) \right) \frac{\sin^2 r}{\pi r^2} e^{(c(b)-r)(u^\circ-1)/T} dr \\
&\quad + x_0^{u^\circ-1} \int_{|r|<c(b)} \left(\varphi(x_0 e^{\frac{c(b)-r}{T}}) - \psi(x_0 \pm 0) \right) \frac{\sin^2 r}{\pi r^2} e^{(c(b)-r)(u^\circ-1)/T} dr \\
&\quad - \Delta \int_{|r|\geq c(b)} \frac{\sin^2 r}{\pi r^2} dr.
\end{aligned}$$

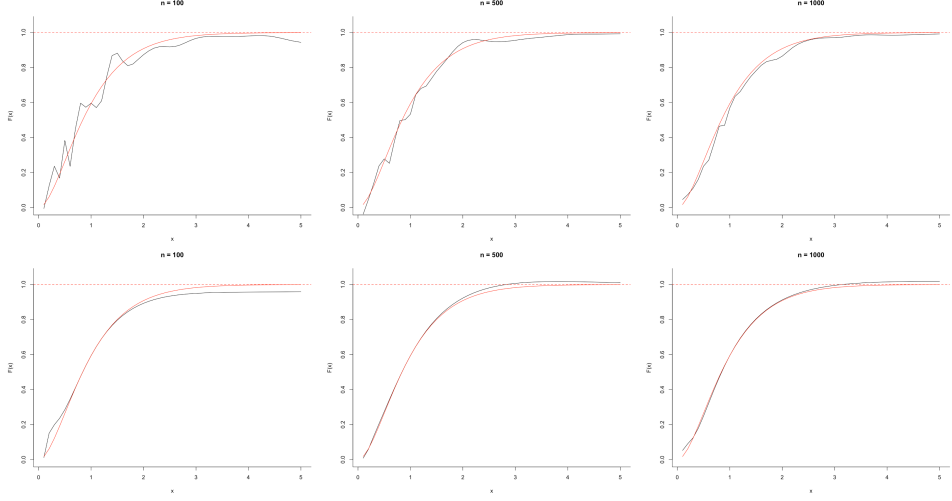


Figure 11: The estimates \hat{F} of the c.d.f. of the $\text{Gamma}(2,2)$ distribution for the estimators (4) based on the Mellin transform (top) and (19) based on the Fourier transform (bottom) superimposed with the true distribution function for G being a c.d.f. of the uniform distribution

Since for any $r < c(b)$, it holds

$$x_0^{u^\circ-1} \left(\varphi(x_0 e^{\frac{c(b)-r}{T}}) - \psi(x_0 \pm 0) \right) \geq x_0^{u^\circ-1} (\varphi(x_0) - \psi(x_0 \pm 0)) = \Delta,$$

we further have

$$\begin{aligned} & x_0^{u^\circ-1} e^{\frac{c(b)(u^\circ-1)}{T}} \left(\tilde{\varphi}(x_0 e^{\frac{c(b)}{T}}) - \tilde{\psi}(x_0 e^{\frac{c(b)}{T}}) \right) \\ & \geq -\frac{x_0^{u^\circ-1}}{\pi} \int_{|r| < c(b)} \left| \psi(x_0 \pm 0) - \psi\left(x_0 e^{\frac{c(b)-r}{T}}\right) \right| e^{(c(b)-r)(u^\circ-1)/T} dr \\ & \quad + \Delta \int_{|r| < c(b)} \frac{\sin^2 r}{\pi r^2} e^{(c(b)-r)(u^\circ-1)/T} dr - \Delta \int_{|r| \geq c(b)} \frac{\sin^2 r}{\pi r^2} dr \\ & \geq -\frac{T}{\pi} x_0^{u^\circ-1} \int_0^{2c(b)/T} \left| \psi(x_0 \pm 0) - \psi(x_0 e^r) \right| dr \\ & \quad + \Delta \int_{|r| < c(b)} \frac{\sin^2 r}{\pi r^2} e^{(c(b)-r)(u^\circ-1)/T} dr - \Delta \int_{|r| \geq c(b)} \frac{\sin^2 r}{\pi r^2} dr. \end{aligned}$$

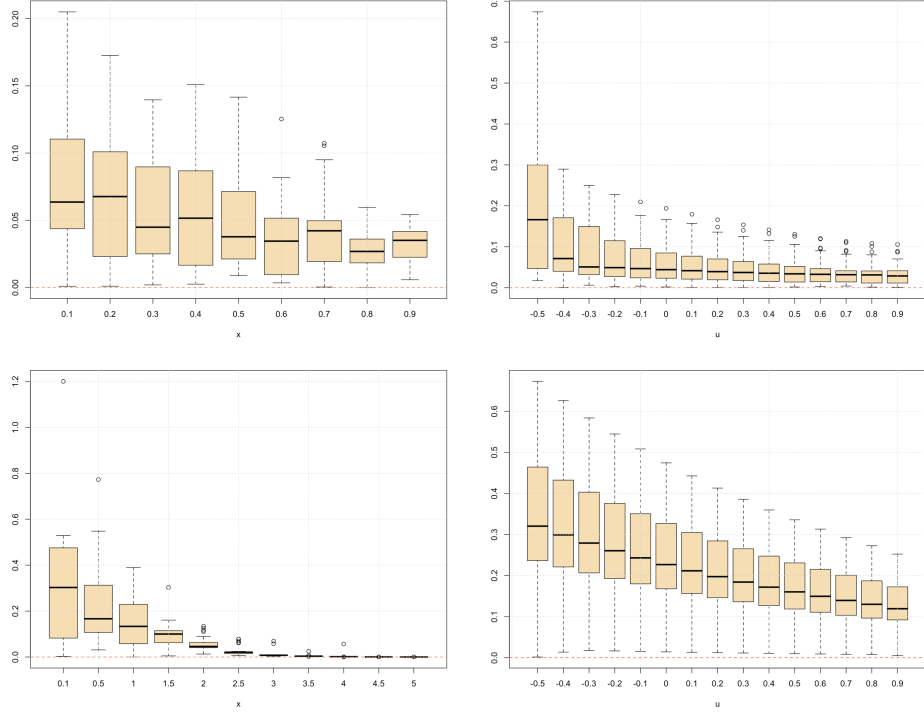


Figure 12: The estimates $\widehat{\mathcal{R}}(\widehat{F}; u^\circ, x)$ for different values of x (left) and u° (right) for Beta(2,2) (top) and Gamma(2,2) (bottom) distributions for G being a c.d.f. of the uniform distribution

Now, noting that

$$\begin{aligned} \int_{|r| < c(b)} \frac{\sin^2 r}{\pi r^2} e^{(c(b)-r)(u^\circ-1)/T} dr &\geq e^{2c(b)(u^\circ-1)/T} \int_{|r| < c(b)} \frac{\sin^2 r}{\pi r^2} dr, \\ \int_{|r| \geq c(b)} \frac{\sin^2 r}{\pi r^2} dr &= 1 - \int_{|r| < c(b)} \frac{\sin^2 r}{\pi r^2} dr \end{aligned}$$

we obtain

$$\begin{aligned} \rho_{u^\circ}(\tilde{\varphi}, \tilde{\psi}) &\geq -\frac{T}{\pi} x_0^{u^\circ-1} \int_0^{2c(b)/T} |\psi(x_0 \pm 0) - \psi(x_0 e^r)| dr \\ &\quad + \Delta \left(-1 + \int_{|r| < c(b)} \frac{\sin^2 r}{\pi r^2} dr \cdot (e^{2c(b)(u^\circ-1)/T} + 1) \right), \end{aligned}$$

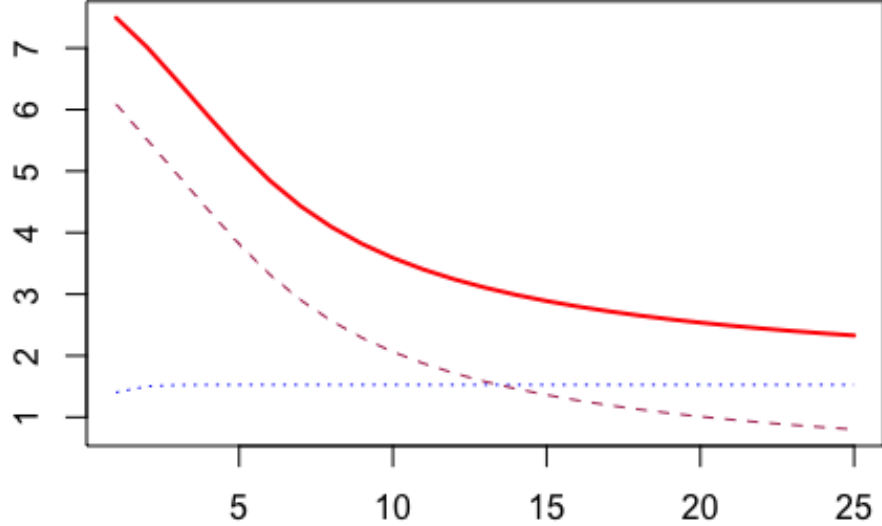


Figure 13: The graphs of the first and the second summands, and the right-hand side in (6), depending on the value of T . The blue dotted line represents the first summand and is for large T is close to 1.1. The maroon dashed line shows the behaviour of the second summand, which tends to 0 as $T \rightarrow \infty$. Finally, the red solid line shows the total behaviour of the r.h.s. in (6).

where $e^{2c(b)(u^\circ-1)/T} + 1 > 3/2$ due to our choice of T . Choosing $c(b)$ as in (7), arrive at the upper bound for Δ

$$\Delta \leq \pi b \cdot \rho_{u^\circ}(\tilde{\varphi}, \tilde{\psi}) + Tb x_0^{u^\circ-1} \int_0^{2c(b)/T} |\psi(x_0 \pm 0) - \psi(x_0 e^r)| dr. \quad (23)$$

Combining this bound with (22), we obtain the result.

B.3 Proof of Theorem 4.1

Let us consider

$$x^{u^\circ-1} |F(x) - \widehat{F}(x)| \leq x^{u^\circ-1} |F(x) - \widetilde{F}(x)| + x^{u^\circ-1} |\widetilde{F}(x) - \widehat{F}(x)| \quad (24)$$

with $\widetilde{F}(x)$ being an auxiliary function defined as the multiplicative convolution

$$\widetilde{F}(x) := F \star W(x) = \int_0^\infty F(x/y) dW(y),$$

where $W : \mathbb{R}_+ \rightarrow \mathbb{R}_+$ is defined by (20). Since $\mathcal{M}[\tilde{F}](z) = \mathcal{M}[F](z)\mathcal{M}[W](z)$ for any z such that $\operatorname{Re}(z) \in \mathcal{C}_{\tilde{F}} = \mathcal{C}_F \cap \mathcal{C}_W$, and $u^\circ \in \mathcal{C}_W$ by (21), we get from Lemma 2.1,

$$\tilde{F}(x) = \frac{1}{2\pi} \int_{-\infty}^{\infty} x^{-u^\circ - \operatorname{i}v + 1} \frac{\mathcal{M}[F](u^\circ + \operatorname{i}v)\mathcal{M}[W](u^\circ + \operatorname{i}v)}{-(u^\circ + \operatorname{i}v - 1)} dv, \quad v \in \mathbb{R}.$$

Noticing that $\mathcal{M}[W](u^\circ + \operatorname{i}v) = K(v)$, see (21), we have for the second summand in (24)

$$\begin{aligned} & x^{u^\circ - 1} |\tilde{F}(x) - \hat{F}(x)| \\ &= x^{u^\circ - 1} \left| \frac{1}{2\pi} \int_{-\infty}^{\infty} x^{(-u^\circ + 1) - \operatorname{i}v} \frac{\mathcal{M}[F](u^\circ + \operatorname{i}v) - \widehat{\mathcal{M}[F]}(u^\circ + \operatorname{i}v)}{-(u^\circ + \operatorname{i}v - 1)} K(v) \right| \\ &= x^{u^\circ - 1} \left| \frac{1}{2\pi n} \sum_{k=1}^n \int_{-\infty}^{\infty} x^{(-u^\circ + 1) - \operatorname{i}v} \frac{\mathcal{M}[F_{\text{mix}}](u^\circ + \operatorname{i}v) - X_k^{(u^\circ - 1) + \operatorname{i}v}}{-(u^\circ + \operatorname{i}v - 1) \mathcal{M}[G](u^\circ + \operatorname{i}v)} K(v) \right| \\ &= \frac{x^{u^\circ - 1}}{2\pi n} \left| \sum_{k=1}^n \Lambda_k(X_k, x) \right|. \end{aligned}$$

As for the first summand in (24), let us note that

$$\begin{aligned} \sup_{x \geq 0} |x^{u^\circ - 1} (F(x) - \tilde{F}(x))| &= \sup_{x \geq 0} \left| x^{u^\circ - 1} F(x) - \int_0^\infty (x/y)^{u^\circ - 1} F(x/y) \tilde{w}(y) dy \right| \\ &= \sup_{x \geq 0} \left| \int_0^\infty \left(x^{u^\circ - 1} F(x) - (x/y)^{u^\circ - 1} F(x/y) \right) \tilde{w}(y) dy \right|, \quad (25) \end{aligned}$$

where $\tilde{w}(y) := w(y)y^{u^\circ - 1}$, $y \in \mathbb{R}_+$ is a density function of some distribution. Since we assume that the distribution function F is continuous at least in a small vicinity of 0, and (9) holds, the supremum in (25) is attained at some point $x_0 > 0$. Thus, by Lemma 3.1,

$$\begin{aligned} x^{u^\circ - 1} |F(x) - \tilde{F}(x)| &\leq \frac{b}{2} \int_{-T}^T \frac{|\mathcal{M}[F](u^\circ + \operatorname{i}v) - \mathcal{M}[\tilde{F}](u^\circ + \operatorname{i}v)|}{|v|} dv \\ &\quad + bT x_0^{u^\circ - 1} \int_0^{2c(b)/T} |F(x_0 \pm 0) - F(x_0 e^r)| dr. \end{aligned}$$

Now it only remains to observe that

$$\begin{aligned} & \int_{-T}^T \frac{|\mathcal{M}[F](u^\circ + iv) - \mathcal{M}[\tilde{F}](u^\circ + iv)|}{|v|} dv \\ &= \int_{-T}^T \frac{|\mathcal{M}[F](u^\circ + iv)(1 - \mathcal{M}[W](u^\circ + iv))|}{|v|} dv = \frac{1}{T} \int_{-T}^T |\mathcal{M}[F](u^\circ + iv)| dv. \end{aligned}$$

B.4 Proof of Theorem 4.2

By the upper bound established in Theorem 4.1,

$$\begin{aligned} \mathcal{R}^*(\hat{F}; u^\circ, x) &\leq \frac{3b^2}{4T^2} \left(\int_{-T}^T |\mathcal{M}[F](u^\circ + iv)| dv \right)^2 \\ &\quad + 3b^2 T^2 x_0^{2(u^\circ-1)} \left(\int_0^{2c(b)/T} |F(x_0 \pm 0) - F(x_0 e^r)| dr \right)^2 \\ &\quad + \frac{3x^{2(u^\circ-1)}}{4\pi^2 n^2} \mathbb{E} \left[\left| \sum_{k=1}^n \Lambda_k(X_k, x) \right|^2 \right]. \end{aligned} \quad (26)$$

Now, since $\Lambda_k(X_k, x)$ are centred i.i.d. for all $k = 1, \dots, n$,

$$\mathbb{E} \left[\left| \sum_{k=1}^n \Lambda_k(X_k, x) \right|^2 \right] = \text{Var} \left(\sum_{k=1}^n \Lambda_k(X_k, x) \right) = n \mathbb{E} \left[\Lambda_1(X_1, x) \overline{\Lambda_1(X_1, x)} \right],$$

where for the latter quantity we have that

$$\begin{aligned} & \mathbb{E} \left[\Lambda_1(X_1, x) \overline{\Lambda_1(X_1, x)} \right] \\ &= \mathbb{E} \left[\int_{-T}^T \int_{-T}^T x^{2(-u^\circ+1)-i(v-w)} \frac{(\mathcal{M}[F_{\text{mix}}](u^\circ + iv) - X_1^{(u^\circ-1)+iv})}{(u^\circ - 1 + iv)(u^\circ - 1 - iw)} \left(1 - \frac{|v|}{T} \right) \right. \\ &\quad \times \left. \frac{(\overline{\mathcal{M}[F_{\text{mix}}](u^\circ + iw)} - X_1^{(u^\circ-1)-iw})}{\mathcal{M}[G](u^\circ + iv) \overline{\mathcal{M}[G](u^\circ + iw)}} \left(1 - \frac{|w|}{T} \right) dv dw \right] \\ &\quad \times x^{2(-u^\circ+1)-i(v-w)} \left(1 - \frac{|v|}{T} \right) \left(1 - \frac{|w|}{T} \right) dv dw. \end{aligned}$$

Since

$$\begin{aligned} & \mathbb{E}[(\mathcal{M}[F_{\text{mix}}](u^\circ + iv) - X_1^{(u^\circ-1)+iv})(\overline{\mathcal{M}[F_{\text{mix}}](u^\circ + iw)} - X_1^{(u^\circ-1)-iw})] \\ &= -\mathcal{M}[F_{\text{mix}}](u^\circ + iv) \mathcal{M}[F_{\text{mix}}](u^\circ - iw) + \mathcal{M}[F_{\text{mix}}](2u^\circ - 1 + i(v - w)), \end{aligned}$$

we further have

$$\begin{aligned}
& \mathbb{E} \left[\Lambda_1(X_1, x) \overline{\Lambda_1(X_1, x)} \right] \\
&= \int_{-T}^T \int_{-T}^T \frac{\mathcal{M}[F_{\text{mix}}](2u^\circ - 1 + i(v - w))}{(u^\circ - 1 + iv)(u^\circ - 1 - iw)\mathcal{M}[G](u^\circ + iv)\overline{\mathcal{M}[G](u^\circ + iw)}} \\
&\quad \times x^{2(-u^\circ + 1) - i(v - w)} \left(1 - \frac{|v|}{T}\right) \left(1 - \frac{|w|}{T}\right) dv dw \\
&- \int_{-T}^T \int_{-T}^T \frac{\mathcal{M}[F_{\text{mix}}](u^\circ + iv)\mathcal{M}[F_{\text{mix}}](u^\circ - iw)}{(u^\circ - 1 + iv)(u^\circ - 1 - iw)\mathcal{M}[G](u^\circ + iv)\overline{\mathcal{M}[G](u^\circ + iw)}} \\
&\quad \times x^{2(-u^\circ + 1) - i(v - w)} \left(1 - \frac{|v|}{T}\right) \left(1 - \frac{|w|}{T}\right) dv dw,
\end{aligned}$$

where the subtrahend is a real positive number. Therefore,

$$\begin{aligned}
& \mathbb{E} \left[\Lambda_1(X_1, x) \overline{\Lambda_1(X_1, x)} \right] \\
&\leq x^{2(-u^\circ + 1)} \int_{-T}^T \int_{-T}^T x^{-i(v - w)} \frac{\sqrt{\mathcal{M}[F_{\text{mix}}](2u^\circ - 1 + i(v - w))}}{(u^\circ - 1 + iv)\mathcal{M}[G](u^\circ + iv)} \left(1 - \frac{|v|}{T}\right) \\
&\quad \times \frac{\sqrt{\mathcal{M}[F_{\text{mix}}](2u^\circ - 1 + i(v - w))}}{(u^\circ - 1 + iw)\mathcal{M}[G](u^\circ + iw)} \left(1 - \frac{|w|}{T}\right) dv dw
\end{aligned}$$

Finally, by the Cauchy-Schwarz inequality,

$$\begin{aligned}
\mathbb{E} \left[\Lambda_1(X_1, x) \overline{\Lambda_1(X_1, x)} \right] &\leq x^{2(-u^\circ+1)} \int_{-T}^T \int_{-T}^T \frac{|\mathcal{M}[F_{\text{mix}}](2u^\circ - 1 + i(v - w))|}{((u^\circ - 1)^2 + v^2) |\mathcal{M}[G](u^\circ + iv)|^2} \\
&\quad \times \left(1 - \frac{|v|}{T} \right)^2 dv dw \\
&\leq x^{2(-u^\circ+1)} \int_{-T}^T \left[\frac{(1 - |v|/T)^2}{((u^\circ - 1)^2 + v^2) |\mathcal{M}[G](u^\circ + iv)|^2} \right. \\
&\quad \times \left. \int_{-\infty}^{\infty} |\mathcal{M}[F_{\text{mix}}](2u^\circ - 1 + i(v - w))| dw \right] dv \\
&\leq x^{2(-u^\circ+1)} \int_{-T}^T \frac{1}{((u^\circ - 1)^2 + v^2) |\mathcal{M}[G](u^\circ + iv)|^2} dv \\
&\quad \times \int_{-\infty}^{\infty} |\mathcal{M}[F_{\text{mix}}](2u^\circ - 1 + iw)| dw.
\end{aligned}$$

Combining the last inequality with (26), we arrive at the desired result.

References

- [1] Asgharian, M., Carone, M. and Fakoor, V. (2012). Large-sample study of the kernel density estimators under multiplicative censoring. *The Annals of Statistics*, 40(1):159–187.
- [2] Belomestny, D. and Goldenshluger, A. (2020). Nonparametric density estimation from observations with multiplicative measurement errors. *Annales de l'Institut Henri Poincaré, Probabilités et Statistiques*, 56(1):36–67.
- [3] Belomestny, D. and Goldenshluger, A. (2021). Density deconvolution under general assumptions on the distribution of measurement errors. *The Annals of Statistics*, 49(2):615–649.
- [4] Belomestny, D. and Panov, V. (2015). Statistical inference for generalized Ornstein-Uhlenbeck processes. *Electronic Journal of Statistics*, 9(2):1974–2006.
- [5] Belomestny, D. and Schoenmakers, J. (2015). Statistical Skorohod embedding problem: Optimality and asymptotic normality. *Statistics & Probability Letters*, 104:169–180.

- [6] Belomestny, D., Comte, F., and Genon – Catalot, V. (2016). Nonparametric Laguerre estimation in the multiplicative censoring model. *Electronic Journal of Statistics*, 10(2):3114–3152.
- [7] Brunel, E., Comte, F. and Genon-Catalot, V. (2016). Nonparametric density and survival function estimation in the multiplicative censoring model. *Test*, 25(3):570–590.
- [8] Comte, F. and Dion, C. (2016). Nonparametric estimation in a multiplicative censoring model with symmetric noise. *Journal of Nonparametric Statistics*, 28(4):768–801.
- [9] Delaigle, A. (2021). Deconvolution kernel density estimation. In *Handbook of Measurement Error Models*, pages 185–220. Chapman and Hall/CRC.
- [10] Fournier, N. and Printems, J. (2010). Absolute continuity for some one-dimensional processes. *Bernoulli*, 16(2):343–360.
- [11] Kawata, T. (1972). *Fourier analysis in probability theory*. Academic Press.
- [12] Lin, Z. and Bai, Z. (2011). *Probability inequalities*. Springer Science & Business Media.
- [13] Lukacs, E. (1970). *Characteristic functions*. Griffin London, Second edition.
- [14] Meister, A. (2009). Deconvolution problems in nonparametric statistics. *Lecture Notes in Statistics, Springer, Berlin, Heidelberg*, pages 5–138.
- [15] Miguel, S., Comte, F. and Johannes, J. (2021). Linear functional estimation under multiplicative measurement errors. *arXiv:2111.14920*.
- [16] Van Es, B., Klaassen, C.A.J., Oudshoorn, K. (2000). Survival analysis under cross-sectional sampling: length bias and multiplicative censoring. *Journal of Statistical Planning and Inference*, 91(2):295–312.
- [17] Van Es, B., Spreij, P., Van Zanten, H. (2003). Nonparametric volatility density estimation. *Bernoulli*, 9(3):451–465.
- [18] Vardi, Y. (1989). Multiplicative censoring, renewal processes, deconvolution and decreasing density: nonparametric estimation. *Biometrika*, 76(4):751–761.
- [19] Zhang, C.-H. (1990). Fourier methods for estimating mixing densities and distributions. *The Annals of Statistics*, pages 806–831.